PERFORMANCE ANALYSIS OF THREE PHASE SQUIRREL CAGE INDUCTION MOTOR WITH DEEP ROTOR BARS IN STEADY-STATE BEHAVIOR

Călin MIHĂILESCU[1], Florin REZMERIȚĂ[2], Ileana CALOMFIRESCU[3], Mihai IORDACHE[4], Nicolae GALAN[5]

The rotor parameters, the resistance and the leakage inductance, vary with the currents frequency of rotor bars due to skin effect, and for small frequencies can be negligible (under 10…15 Hz); but for higher frequencies (e.g. 50Hz) this variation of the parameters cannot be negligible. In this paperwork, for higher frequencies some analytic expressions are proposed, that results from the skin effect theory, for the rotor resistance and for the leakage inductance. The simulations were done by SYMNAP – SYmbolic Modified Nodal Analysis Program, a program that can determine, in a full-symbolic form the voltages and the currents for the equivalent scheme for one phase of the asynchronous motor in steady-state behavior. Symbolic expressions for the characteristics quantities of the steady-state behavior of the induction motor allow graphic representation for different parameters. These analytic expressions allow a more accurate analysis of asynchronous motor performance for different drive systems. It was found that the nominal values of the quantities that characterize the induction motor operation, obtained by simulation, have near values to the ones from the catalogue.

Keywords: Modified nodal equations, induction motor, steady-state (sinusoidal) behaviour, skin effect, sensitivity

1. Introduction

Numerous studies have been made on estimating the electrical parameters of the asynchronous machine given both skin effect, and the saturation level, [1-9]. For the electrical drives with three phase induction, motors with deep rotor bar were developed mathematical models and command strategies for developing high performance systems, [6]. In electrical drives, it is preferred the vector command in respect to the rotor flux, a flux that cannot be defined using one form for motor with deep rotor bars; as a result, in many cases it is used the air gap flux

[1] Electrical Engineering Faculty, University POLITEHNICA din Bucharest, Romania
[2] Electrical Engineering Faculty, University POLITEHNICA din Bucharest, Romania
[3] Electrical Engineering Faculty, University POLITEHNICA din Bucharest, Romania, e-mail: ileana.calomfirescu@yahoo.co.uk
[4] Electrical Engineering Faculty, University POLITEHNICA din Bucharest, Romania
[5] Electrical Engineering Faculty, University POLITEHNICA din Bucharest, Romania

for the vector command. The squirrel cage with deep rotor bar can be equivalent with a double cage, one of these cages being with constant parameters [8].

Based on the influence of the skin effect over electrical rotor parameters can be constructed a mathematical model for the asynchronous motor with deep rotor bar, that allows simulation of different operating modes, which are presented in this paperwork. It is considered constant stator current frequency, equal to the network frequency at which the motor is fed. Rotor parameters are considered constant, independent of the rotor current frequency, for values between 0 and 10...15 Hz. For higher frequencies, analytic expressions are proposed, that result from the skin effect theory, for the rotor resistance and leakage inductance. In sinusoidal steady-state, simulations were performed by the **SYMNAP** – **SY**mbolic **M**odified **N**odal **A**nalysis, [10], a program that allows complete symbolic determination of the branch voltages and currents of the equivalent scheme corresponding to one phase of the induction motor. The paper also presents an improvement of sensitivity analysis method**.** The circuit sensitivities are computed by means of the derivates of the circuit transfer functions. The equivalent circuit sensitivity analysis of induction motor aims to identify the critical circuit elements allowing the comparison of different circuit structure and selecting the proper circuit for a specified application. Also, the sensitivities are very useful in the identification parameters of the induction motor. In [11] it is presented the performance analysis of three phase-squirrel cage induction motor with deep rotor bars *in transient behavior*.

2. Simulation of the Induction Motor in Steady-State Behavior

In order to analyze the steady-state behavior of the induction motor the modified nodal equations in the full-symbolic form are used. In this case the equivalent circuit corresponding to one induction motor phase is used (Fig. 1). Simulation for the asynchronous motor for the stabilized conditions is done in two steps: 1) rotor parameters are considered constants; 2) rotor parameters variables corresponding with the variation frequency of the rotor currents (we take into consideration the skin effect for the rotor currents);

The circuit in Fig. 1 contains a time-variable resistor depending of the electrical slip – R_5 resistor. In order to formulate the modified nodal equations in full-symbolic form, we use an original computing program called SYMNAP – SYmbolic Modified Nodal Analysis Program, [10].

2.1. Rotor Electrical Parameters

The skin effect analysis shows that the rotor resistance $R_r^{'}$ reported at the stator increases with $\sqrt{\omega_r}$, and leakage inductance $L_{r\sigma}^{'}$ decreases with $\sqrt{\omega_r}$, when

ω_r is the rotor angular frequency, [13]. Therefore, the rotor parameters reported at the stator can be written as it follows, [13]:

$$\begin{aligned} R_r'(\omega_r) &= R_r' = ct.\ for\ \ \omega_r \in (0;\omega_{rx}); \\ R_r'(\omega_r) &= K_1 + K_2\sqrt{\omega_r};\ \text{for}\ \ \omega_r > \omega_{rx}. \\ L_r'(\omega_r) &= L_r' = ct.\ for\ \ \omega_r \in (0;\omega_{rx}); \\ L_{r\sigma}'(\omega_r) &= L_{r\sigma}' = ct.\ for\quad \omega_r \in (0;\omega_{rx}); \\ L_{r\sigma}'(\omega_r) &= K_3 - \frac{K_4}{\sqrt{\omega_r}};\quad \omega_r > \omega_{rx}. \end{aligned} \tag{1}$$

The inductance $L_r'(\omega_r)$ is cyclic rotor inductance and constants K_1, K_2, K_3 and K_4 are determined from the continuity condition at the point $\omega_r = \omega_{rx}$ and calculation of the electrical parameters for the squirrel cage at starting point (a = 1, it is denoted the slip by the letter a), these parameters are obtained from the catalogue data. Till the rotor angular frequency is $\omega_r = \omega_{rx}$, the rotor parameters are considered constant, and for $\omega_r \geq \omega_{rx}$ the rotor parameters vary with the rotor angular frequency ω_r according to relations (1). These are valid for a wide range of frequencies from rotor circuit.

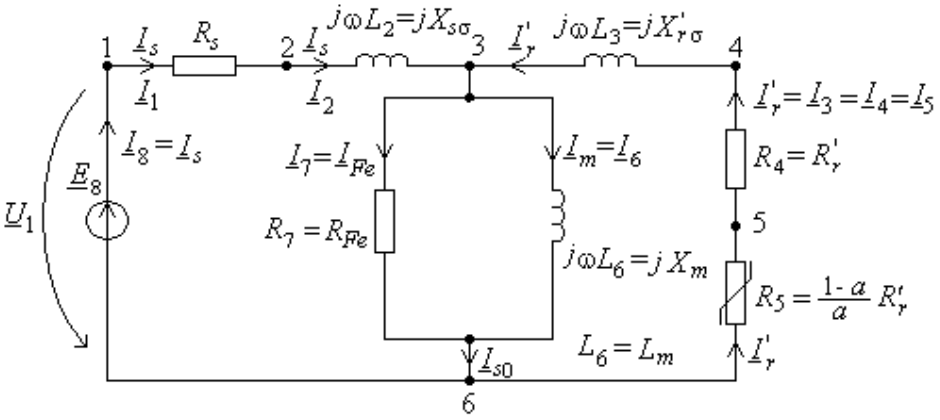

Fig.1. Induction motor equivalent scheme

2.1.1. Rotor Parameters at Starting Point

Rotor squirrel cage is made with deep bars, parameters R_r' and $L_{r\sigma}'$ vary in large limits when the rotor angular frequency ω_r takes values between 0 and ω_1; at the starting point ($\Omega = 0$), the rotor angular frequency ω_r is equal to the stator angular frequency ω_1, in this case the skin effect is strong ($\omega_1 = 2\cdot\pi\cdot 50$,

$$f_{rn} = 50 \cdot a_n = 0{,}75 \text{ Hz}; \frac{\left(R_r^i\right)_{f_r=50}}{\left(R_r^i\right)_{f_{rn}}} = 2{,}13; \ \frac{\left(L_r^i\right)_{f_r=50}}{\left(L_r^i\right)_{f_{rn}}} = 0{,}989) .$$

Based on the catalogue data the following quantities can be calculated: P_{1n}, a_n, M_n and S_n.

Next step for the calculation of the starting parameters is: the starting impedance Z_p, the rotor resistance at starting point R'_{rp} and the leakage inductance at staring point $L'_{rp\sigma}$. In the computation process, the rated impedance Z_n is used. Using the known relations from the asynchronous motor theory, for Ω = 0 - starting point, the rotor resistance R'_{rp} is computation thus, [11]:

$$\begin{aligned}
&a = 1 \Rightarrow \omega_r = \omega_1 \Rightarrow Z_p = \frac{U_{fn}}{I_p} = \frac{U_{fn}}{i_{pn} I_{fn}} = \frac{Z_n}{i_p}; \\
&Z_p = \frac{U_{fn}}{I_p} = \frac{U_{fn}}{i_{pn} I_{fn}} = \frac{Z_n}{i_p}; \ Z_n = \frac{U_{fn}}{I_{fn}}; \\
&M = \frac{P_{Jr}}{\Omega_1 a} = \frac{3 R'_{rp} I'^{\,2}_{rp}}{\Omega_1};
\end{aligned} \tag{2a}$$

where: P_{Jr} - represents Joule loss in rotor circuit, and Ω_1 - is synchronous angular speed.

At starting point, the slip has value of 1, and it can be calculated the rotor resistance R'_{rp} as follows:

$$\begin{aligned}
&a = 1 \Rightarrow M_p = \frac{3 R'_{rp} I'^{2}_{rp}}{\Omega_1} \cong \frac{3 R'_{rp} I^2_{sp}}{\Omega_1}; \\
&\left(I_{s0} \cong 0 \Rightarrow I'_{rp} \cong I_{sp}\right); \\
&\frac{M_p}{M_n} = m_p \cong \frac{3 R'_{rp} I^2_{sp}}{\Omega_1 M_n} \frac{\Omega_n}{\Omega_n} = \frac{3 R'_{rp} I^2_{sp}}{P_n} \left(1 - a_n\right) \Rightarrow \\
&R'_{rp} = \frac{m_p P_n}{3\left(1 - a_n\right)\left(i_p I_{fn}\right)^2}.
\end{aligned} \tag{2b}$$

The values of the parameters are: Z_p - starting impedance, R_s - resistance of the stator winding, $L_{s\sigma}$ - leakage inductance of stator winding, and $L'_{rp\sigma}$ is the leakage inductance of rotor winding at the starting point. This leakage inductance can be computed with the following relation:

$$\begin{aligned} &a=1\Rightarrow \\ &X_{p\sigma}=\omega_1 L_{p\sigma}=\omega_1(L_{s\sigma}+L_{rp\sigma}{}')=\sqrt{Z_p^2-(R_s+c_1R'_{rp})^2}; \\ &c_1\cong 1\Rightarrow L_{rp\sigma}{}'=\frac{\sqrt{Z_p^2-(R_s+R'_{rp})^2}}{\omega_1}-L_{s\sigma}. \end{aligned} \tag{3}$$

At this stage, in the absence of the skin effect the parameters R'_r and $L'_{r\sigma}$ are known and if skin effect is taken into account, we will use the parameters R'_{rp}, $L'_{rp\sigma}$. The calculation of the K_1, K_2, K_3 and K_4 constants leads to the next relations for R'_r-rotor resistance (4a) and $L'_{r\sigma}$-rotor leakage inductance (4b), [11]:

$$R_r{}'(\omega_r)=\begin{cases} R'_r;\ \omega_r\in[0;\omega_{rx}] \\ \dfrac{R'_r\sqrt{\omega_1}-R'_{rp}\sqrt{\omega_{rx}}}{\sqrt{\omega_1}-\sqrt{\omega_{rx}}}+\dfrac{R'_{rp}-R'_r}{\sqrt{\omega_1}-\sqrt{\omega_{rx}}}\sqrt{\omega_r};\ \sqrt{\omega_r}>\sqrt{\omega_{rx}} \end{cases} \tag{4a}$$

$$\begin{aligned} &L'_{r\sigma}(\omega_r)=\begin{cases} L'_{r\sigma};\quad \omega_r\in[0;\omega_{rx}] \\ \dfrac{\sqrt{\omega_{rx}}\,L'_{r\sigma}-\sqrt{\omega_1}\,L'_{rp\sigma}}{\sqrt{\omega_{rx}}-\sqrt{\omega_1}}-\dfrac{(L'_{r\sigma}-L'_{rp\sigma})\sqrt{\omega_1}\sqrt{\omega_{rx}}}{\sqrt{\omega_{rx}}-\sqrt{\omega_1}}\dfrac{1}{\sqrt{\omega_r}};\ \sqrt{\omega_r}>\sqrt{\omega_{rx}}; \end{cases} \\ &L'_r=L'_{r\sigma}(\omega_r)+L_\mu; \end{aligned} \tag{4b}$$

where $L_\mu=ct$ is the magnetizing inductance.

The last two relations in system (4) highlight the variation of the rotor parameters $R'_r(\omega_r)$ and $L'_{r\sigma}(\omega_r)$ in respect of the ω_r, due to skin effect. The mathematical structure of the model (1), remains the same, except that the parameters R'_r and $L'_{r\sigma}$ become $R'_r(\omega_r)$, and $L'_{r\sigma}(\omega_r)$, respectively, according to relations (4a) and (4b).

For the relative rotor resistance reported to the stator r'_r we can prove a very simple formula, as it follows:

$$R_r^{'} = \frac{a_n (P)_n}{3I_r^{'2}} = \frac{a_n (P_M)_n}{3I_r^{'2}(1-a_n)} = \frac{a_n (P_n + P_{vf})}{3I_r^{'2}(1-a_n)} \cong$$
$$\cong \frac{a_n P_n}{3I_r^{'2}(1-a_n)} \cong a_n \frac{\eta_n 3U_{sn} I_{sn} \cos\varphi_{sn}}{3(I_{sn}\cos\varphi_{sn})^2 (1-a_n)} \Rightarrow$$
$$\Rightarrow \frac{R_r^{'}}{Z_b} = R_r^{'} \frac{I_{sn}}{U_{sn}} = r_r^{'} = a_n \frac{\eta_n}{(1-a_n)\cos\varphi_{sn}};\ Z_b = \frac{U_{fn}}{I_{fn}}. \quad (5)$$
$$\frac{\eta_n}{(1-a_n)\cos\varphi_{sn}} = 1{,}128.$$

Even if the expression $\frac{\eta_n}{(1-a_n)\cos\varphi_{sn}}$ has the value 1,128, at the beginning computing we can consider $r_r^{'} = \frac{R_r^{'}}{Z_b} \cong a_n$.

2.2. The Study of Asynchronous Three Phase Motor with Known Parameters

We have studied an engine produced in Romania, because we obtained all the catalogue data, which is highly unusual for the engines produced in Europe. In order to simulate different operating behaviors of the three phase asynchronous motor expressions obtained in section 2.1 we will use the rated values presented in table 1:

Table 1

Rated Values for the Motor

P_n kW	U_n V	I_n A	Ω_1 rad/s	Ω rad/s	η_n %	$\cos\varphi_{1n}$ -	i_p -	m_p -	m_n -	J kgm^2	Connection
110	400	198	104,72	103,15	94,5	0,85	6,7	2	2,2	3,38	star

U_{fn} = 231V; I_{fn} = 198 A; $Z_b = Z_n = U_{fn}/ I_{fn}$ = 1,168 Ω ; f_n = 50 Hz ; p = 3; $R_1 = R_s$ = 0,025 Ω ; $R_4 = R_r^{'}$ = 0,01812 Ω ; $L_2 = L_{s\sigma}$ = 0,52 mH; $L_3 = L_{r\sigma}^{'}$ = 0,48 mH ; $L_m = L_8 = L_\mu$ = 15 mH , and $R_7 = R_{Fe}$ = 100 Ω.

With the values from table 1 the next quantities are calculated: M_n = 1067 Nm ; M_p = 2134 Nm; I_p = 1326,6 A; S_n = 137214 VA; a_n =0,015; $P_{1n} = S_n \cdot \cos\varphi_{1n}$ = 116632 W; $r_r^{'}$ = 0,0 155 ≅ a_n = 0,015 (the error is 3,33%).

It can be noticed that the last relation (5) is verified with a very good approximation.

Based on relations (3) and the data in table 2, we obtain the numerical values for the electrical parameters reported to the rotor cage for ω_{rx} = 81 rad/s; where electrical parameters of the motor are:

$$L_s = 0{,}01552 \text{ H};\ R_s = 0{,}025\Omega;\ L_\mu = 0{,}015 \text{ H}$$

$$L'_{r\sigma} = \begin{cases} 0{,}00048 \text{ H}; & \omega_r \in [0;81] \\ -0{,}00042 + 0{,}0081\dfrac{1}{\sqrt{\omega_r}}; & [81;100\pi]; \end{cases} \tag{6}$$

$$R'_r(\omega_r) = \begin{cases} 0{,}01812\omega_r \in [0;81] \\ -0{,}0069 + 0{,}00278\sqrt{\omega_r}; [81;100\pi] \end{cases}$$

The rotor cyclic inductance is expressed, based on catalog data of asynchronous motor, as:

$$L'_r = 0.015 + \begin{cases} 0{,}00048 \text{ H}; \omega_r \in [0;81] \\ -0{,}00042 + 0{,}0081\dfrac{1}{\sqrt{\omega_r}}. \\ \omega_r \in [81;100\pi] \end{cases} \tag{7}$$

With these data we can make any simulation for the motor in any working behavior.

For motor with the data sheet from table 1, the time constants are:

$$T_s = \frac{L_s}{R_s} = 0{,}6208; \quad T'_s = \sigma T_s = 0{,}0394\ s$$

$$T_r = \frac{L'_r}{R'_r} = 0{,}854; \quad T'_r = \sigma T_r = 0{,}0542\ s \tag{8}$$

$$T_{mec} = \frac{J}{M_m}\Omega_1 = 0{,}151 \quad s, \quad \sigma = 1 - \frac{L_\mu^2}{L_s L'_r}$$

where: T_s – is the time constant of the stator winding; σ - total leakage coefficient; T'_s – represents the transient time constant of the stator winding; T_r – is the time constant of the rotor winding; T'_r – is the transient time constant for the rotor winding, and T_{mec} - is the mechanical constant of the motor. The stator time constants are greater than the rotor time constants. Therefore, the transient behavior in the stator windings will take more time than the transient behavior in the rotor windings.

Running the SYMNAP we obtain the following modified nodal equations in full symbolic form:

The independent variables

$$[V_1, V_2, V_3, V_4, V_5, I_8]^t$$

Equation system

$(1/R_s)*V_1 + (-1/R_s)*V_2 + (-1)*I_8 = 0;$

$(-1/R_s)*V_1 + (1/R_s+1/(s*L_s))*V_2 +$

$(-1/(s*L_s))*V_3=0;$

$(-1/(s*L_s))*V_2 +(1/(s*L_s)+1/(s*L_r)+1/(s*L_m)+1/(R_{Fe}))*V_3 + (-1/(s*L_r))*V_4 = 0;$

+ (-1/(s*Lr))*V3 + (+1/(s*Lr)+1/(Rr))*V4 + (-1/(Rr))*V5 = 0;

$(-1/(R_r))*V_4 + (1/(R_r)+1/(R_r*(1-a)/a))*V_5 = 0;$

$(-1)*V_1 = - E_{8,}$

where: V_1, V_2, V_3, V_4 and V_5 are the electric potentials corresponding to the circuits nodes, I_8 represents the current through of independent voltage source E_8 (these are the independent variables in the modified nodal method), a is the electrical slip and s is Laplace operator in the SYMNAP software.

For an induction motor with the nominal data presented above, we obtained the following results:

1. Expression of the electromagnetic torque in function of the slip a

$$M\_cp\_a := \frac{0.183\ 10^{13}\ a}{0.677\ 10^{10}\ a^2 + 0.611\ 10^{8}\ a + 0.232\ 10^{8}}$$

when the rotor parameters are considered constants, and

$$\begin{aligned} M\_vp\_a :=\ & 0.426\ 10^{11}\ (-0.0069 + 0.0492\ \sqrt{a}\ )\ |a|^3 \Big/ ((\\ & 300000.\ |a|^{(3/2)} \cos(-2.36 + 2.36\ \mathrm{signum}(a))\ a \\ & + 496.\ |a| \cos(-2.36 + 2.36\ \mathrm{signum}(a))\ a + 19900.\ a^{(3/2)} \sqrt{\mathrm{signum}(a)} \\ & - 130000.\ a\,|a|^{(3/2)} \sin(-2.36 + 2.36\ \mathrm{signum}(a)) \\ & - 10500.\ |a| \sin(-2.36 + 2.36\ \mathrm{signum}(a))\ a \\ & - 10500.\ |a|^2 \cos(-2.36 + 2.36\ \mathrm{signum}(a)) + 702000.\ a^2 - 40600.\ a\sqrt{|a|} + 729.\ |a| \\ & - 496.\ |a|^2 \sin(-2.36 + 2.36\ \mathrm{signum}(a)) + 729.\ \mathrm{signum}(a)\ a + 38200.\ |a|^3)\ a) \end{aligned}$$

for the case we take into account the skin effect.

2. The currents, losses, electromagnetic torques and slips, obtained by simulation, are presented in the Table no 2.

Table 2

$a_n = 0{,}015$ $a_1 = \frac{\omega_{rx}}{\omega_1} = 0{,}26$ $I_{sn} = 190{,}86$ A $I'_{rn} = 175{,}73$ A $I_{Lmn} = 45{,}42$ A $I_{RFen} = 4{,}278$ A $i_p = \frac{I_{sn}}{I_{Lmn}} = 4{,}2$ $M_n = 1069{,}2$ Nm $M_m = 2141{,}422$ Nm	$M_p = 1828{,}468$ Nm $P_{mecn} = 110230$ W $P_{Cu1n} = 2732{,}21$ W $P_{Cu2n} = 1678{,}63$ W $P_{RFen} = 5491{,}596$ W $a_{cr} = 0{,}05856$ $r_{a_{cr}\_a_n} = \frac{a_{cr}}{a_n} = 3{,}9$ $m_m = \frac{M_m}{M_n} = 2{,}003$ $m_p = \frac{M_p}{M_n} = 1{,}71$ $i_p = \frac{I_{fp}}{I_{fn}} = 4{,}2$

The above results have near values to the ones from the catalogue.

In Figs. 2, 3, and 4 are represented the variations of the electromagnetic torque, currents, and the losses, respectively, with respect with the slip.

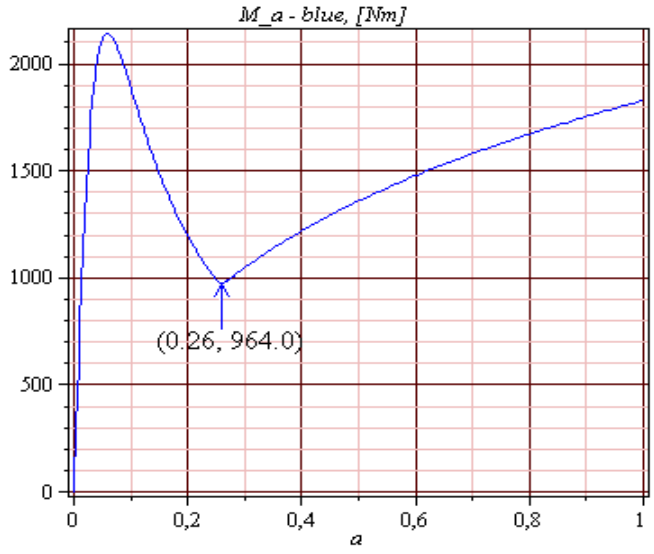

Fig. 2. Variation of electromagnetic torque – slip

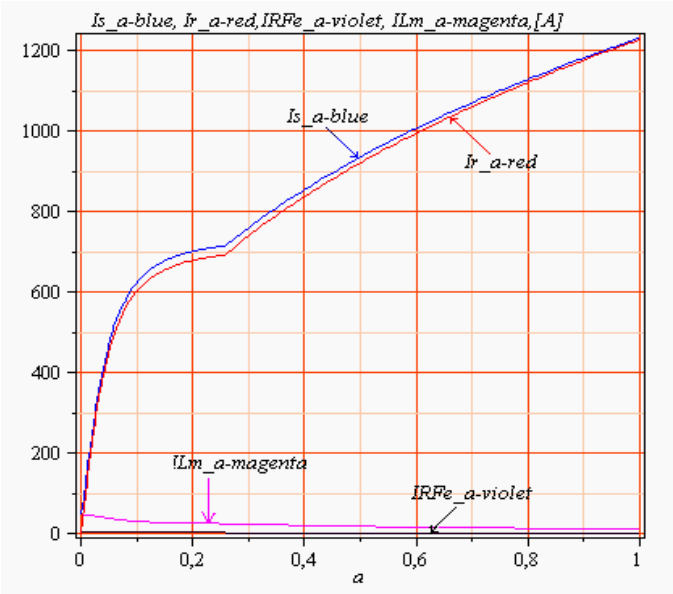

Fig. 3. Variation of currents –slip

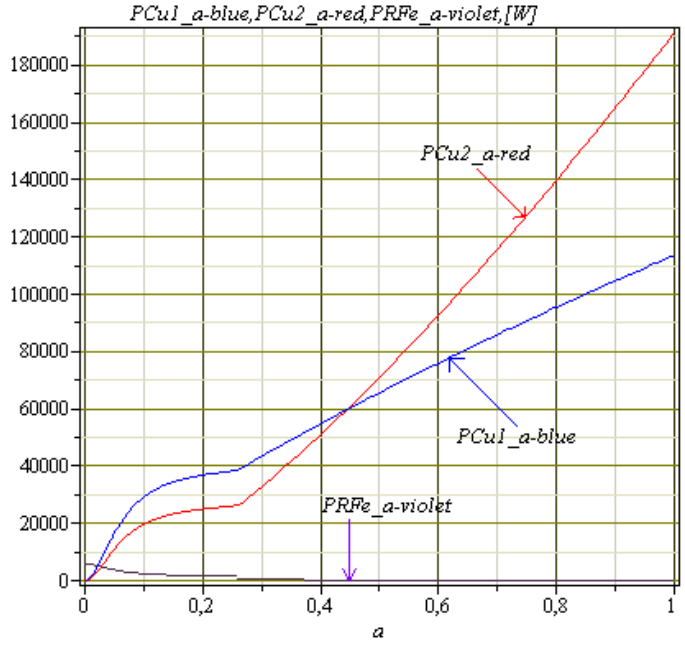

Fig. 4. Variation of losses –slip.

In Fig. 5 is shown the variation of the electromagnetic torque vs. rotor angular frequency.

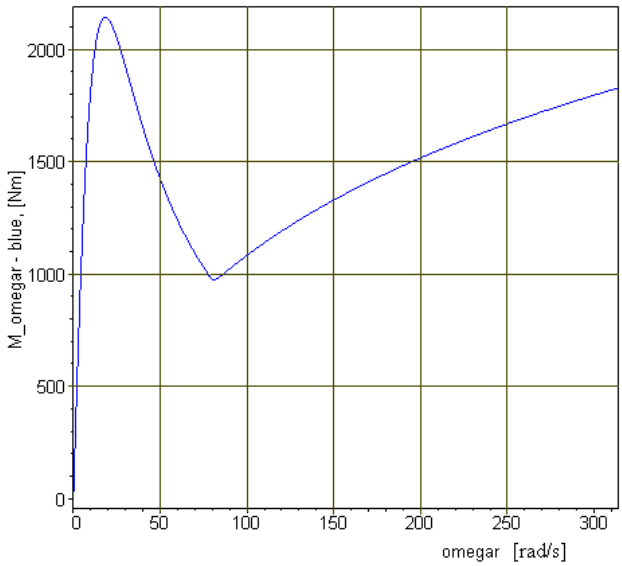

Fig. 5. Variation of electromagnetic torque – rotor pulsation

3. Sensitivity study

We plan to compute the input impedance sensitivity in complex value $\underline{Z}_{ii} = \underline{U}_1/\underline{I}_1 = \underline{Z}_{1\_5\_1\_5}$ .To do that is necessary to generate in full symbolic form this transfer relation. After computing with **SYMNAP** programm we get the $\underline{Z}_{ii}$ *relation*

$$Z1\_5\_1\_5\_f := (-247.673152\, I f^3\, L2\, L3\, L6\, a - 39.4384\, (L6\, a\, L3\, R5 + L2\, L6\, a\, R5 + L6\, a\, L3\, R1 + L2\, a\, L3\, R5 + L2\, L6\, R2)\, f^2 + 6.28\, I\, (L6\, R5\, R2 + L2\, R5\, R2 + L6\, a\, R1\, R5 + L6\, R1\, R2 + a\, L3\, R1\, R5)\, f + R1\, R5\, R2) \,/\, (-39.4384\, f^2\, L6\, a\, L3 + 6.28\, I\, (L6\, a\, R5 + L6\, R2 + a\, L3\, R5)\, f + R5\, R2)$$

- a is slip and f is frequency.

To compute the normalized sensitivity of input impedance $\underline{Z}_{ii}$ rated to x parameter we use the following formula:

$$\underline{S}_x^{\underline{Z}_{ii}} \overset{d}{=} \frac{\partial \underline{Z}_{ii}}{\partial x} \cdot \frac{x}{\underline{Z}_{ii}} \tag{9}$$

The normalized sensitivity of the input impedance module is the real value of the formula (9) and imaginary value represents the imaginary value of the same formula. In Figs. 6 and 7 there are represented the variations with frequency of the normalized rated sensitivity to all motor's parameters, in Fig. 6 the module sensitivity and in Fig. 7 the module phase.

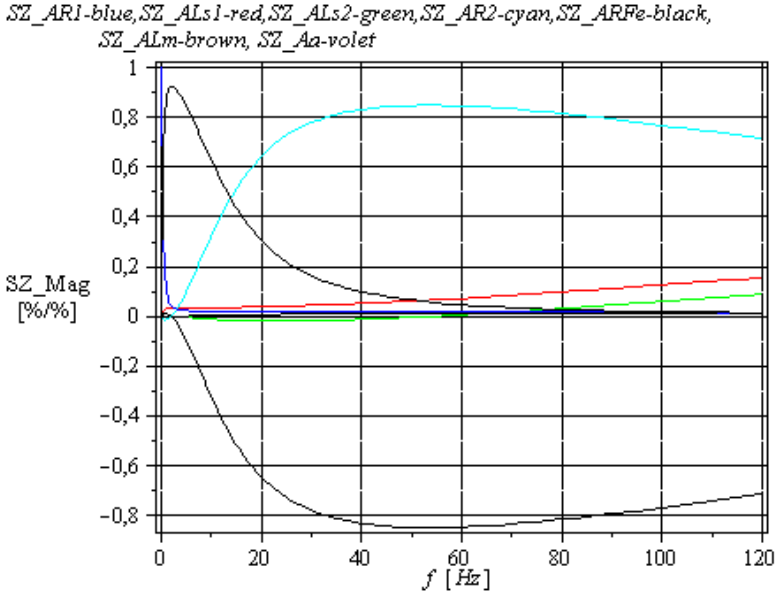

Fig. 6. The variations with frequency of the normalized rated sensitivity to all motor's parameters

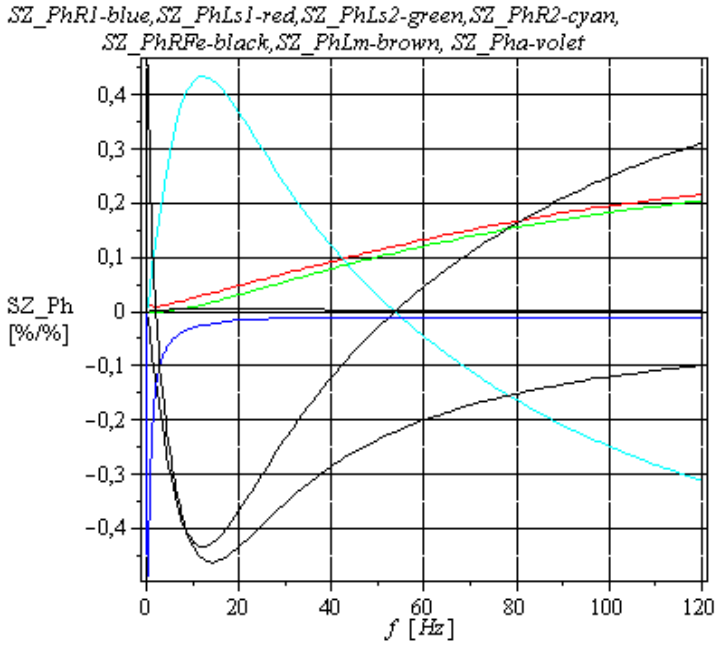

Fig. 7. The variations with phase of the normalized rated sensitivity frequency to all motor's parameters

From Figs. 6 and 7, we can identify the critical parameters of asynchronous motor – the ones with the highest sensitivity rates. For example, the *SZ_PhR*1 quantity represents the normalized sensitivity of the driving point impedance phase in respect to the R_1 parameter.

In Figs. 6 and 7 we consider the frequency variation till 120 Hz, because in the case when the induction motor works in the break behaviour , the frequency becomes equal to the double of the rated frequency.

6. Conclusions

This paperwork presents the influence of skin effect on the electrical parameters of the rotor and on this basis is constructed the mathematical model of the asynchronous machine with deep bars that allows simulation of steady-state behavior. Initial, the stator currents frequency is considered constant, equal to the network frequency. In fact, rotor parameters are considered constants, independent of the rotor frequency, for rotor frequency values between 0 and 10…15 Hz. For higher frequencies, analytic expressions are proposed, resulting from skin effect theory, both for the rotor resistance and the leakage inductance. The asynchronous motor simulations in sinusoidal steady state were performed with the program the **SYMNAP** – **SY**mbolic **M**odified **N**odal **A**nalysis, a program that can determine in a full- symbolic form the voltages and the currents for the equivalent scheme for one phase of the asynchronous motor. Symbolic expressions for the characteristics quantities of the general regime of the induction motor allow graphic representation for different parameters.

The induction motor equivalent circuit sensitivity analysis aims to identify the critical circuit elements allowing the comparison of different circuit structure and selecting the proper circuit for a specified application. Also, the sensitivities are very useful in the identification of the induction motor parameters; a parameter that has a small sensitivity is much more difficult to identify then a parameter with a large value of the sensitivity.

Acknowledgment

This work was supported by the Sectorial Operational Program - Human Resources Development 2007-2013 of the Romanian Ministry of Labor, Family and Social Protection through the Financial Agreement POSDRU/88/1.5/S/61178

R E F E R E N C E S

[1] *A.-K. Repo, P. Rasilo, a. A. Arkkio*, Dynamic electromagnetic torque model and parameter estimation for a deep-bar induction machine, IET Electr. Power Appl., **vol. 2**, No. 3, pp. 183 - 192, 2008.

[2] *Levi E.,* Main flux saturation modelling in double-cage and deep-bar induction machines, IEEE Trans. Energy Conversion, **vol. 11**, No. 2, pp.305 – 311, 1996.

[3] *K.S. Huang, Q.H. Wu, D.R. Turner*, Effective Identification of Induction Motor Parameters Based on Fewer Measurements. IEEE Trans. Energy Converssion, **vol. 17**, No. 1, pp.305 – 311, pp. 55 – 59, 2002.

[4] *D.J.Atkinson, J.W. Finch, P.P.Acarnley*, Estimation of rotor resistance in induction motors, IEE Proc. Electr. Power Appl., **vol. 143**, no.1, pp. 87 -94, 1996.â

[5] *J. Pedra, L Sainz*, Parameter estimation of squirrel-cage induction motors without torque measurements, IEE Proc. Electr. Power Appl., **vol. 153**, no.2, pp. 87 -94, 2006.

[6] *Rik W.A.A. De Doncker*, Field-Oriented Controllers with Rotor Deep Bar Compensation Circuits, IEEE Trans. Industry Applications, **vol. 28**, nr. 5 , pp. 1062 – 1070, 1992.

[7] *Aurel Câmpeanu*, Introducere în dinamica maşinilor electrice de curent alternativ (Introduction in Dynamic of Electrical Machines in Alternanting Curent), Editura Academiei Române, Bucureşti, 1998.

[8] *Jul-Ki Seok, Seung-Ki Sul*, Pseudorotor-Flux-Oriented Control of an Induction Machine for Deep-Bar-E ffect Compensation, IEEE Trans. Industry Applications, **vol. 34**, nr. 3 , pp. 429 – 434 , 1998.

[9] *Alexander C. Smith, Russell C. Healez, Stephen Williamson*, A Transient Induction Motor Model Including Saturation and Deep Bar Effect, IEEE Trans. Energy Converssion, **vol. 11**, No. 1, pp.8 -15, 1996.

[10] *M. Iordache, Lucia Dumitriu*, **SYMNAP** – **SY**mbolic **M**odified **N**odal **A**nalysis, User Guide, Library of Electrical Department, PUB, Bucharest, 2000.

[11] *C. Mihăilescu, Fl. Rezmeriță, Ileana Calomfirescu, M. Iordache, N. Galan*, Performance Analysis of Three Phase-Squirred Cage Induction Motor with Deep Rotor Bars in Transient Behavior, Electrical and Electronic Engineering, p-ISSN:2162-9455 e-ISSN: 2162-8459, **vol. 2**, No. 2, 2012, pp. 11-17.

[12] *Neculai Galan*, Manşini Electrice (Electrical Machines), Editura Academiei Române, Bucureşti, 2011.